Soft Matter

PAPER

View Article Online
View Journal | View Issue

Cite this: *Soft Matter*, 2017, 13, 2239

Received 25th January 2017,
Accepted 23rd February 2017

DOI: 10.1039/c7sm00195a

rsc.li/soft-matter-journal

Switchable surface structured hydrogel coatings

Sander Kommeren,*[a] J. Dongmo[b] and C. W. M. Bastiaansen[ac]

Switchable surface structures based on hydrogels are an emerging field in material science, microfluidics, soft robotics and anti-fouling. Here, we describe a novel method that uses a photo-cross-linkable terpolymer to create a hydrogel coating with a switchable surface structure. The terpolymer is based on poly(*N*-isopropylacrylamide) (PNIPAm) and it is shown that simple coating technologies like slit die coating can be used under ambient conditions. It is also shown that the swelling ratio of the coating is controlled by the energy dose of ultraviolet (UV) light. Simple and complex surface structures were created using respectively single or multiple UV illumination steps through masks and it is shown that the hydrogel coatings can be reversibly switched from a structured state to a flat state with temperature.

1. Introduction

Shape changing surfaces have been of considerable interest in a variety of different fields and for various purposes (*e.g.*, optical manipulation,[1] environmental sensing[2,3] and friction control[4]). Stimuli responsive hydrogels are one class of materials that can be used to create these shape-changing surfaces. These stimuli responsive hydrogels can switch between a swollen and collapsed state in response to environmental changes that include for example, humidity,[5,6] pH,[7,8] temperature[8–10] or light.[11–14] Hydrogels operate in an aqueous environment and therefore they have potential applications in microfluidic devices[8,15,16] or for cell cultivation surfaces.[17–21]

Hydrogels with static microstructured surfaces are of interest in cell behaviour studies during cultivation.[20,22] However cells constantly interact and changes it surroundings, like topography. For a better understanding of the cell behaviour to these changes in topography, dynamic hydrogel surfaces have also been investigated.[21] Surfaces that are able to switch their topographies are not only of interest in cell behaviour studies, but also in protein absorption studies,[23] tunable wettability,[24] microfluidic applications[15,16,25] and photonic sensors.[26]

A well-known stimuli responsive polymer is poly(*N*-isopropylacrylamide) (PNIPAm). PNIPAm is a temperature responsive polymer that undergoes a phase transition at roughly 32 °C, also known as the lower critical solution temperature (LCST).[27] This phase transition has been attributed to hydrogen-bonding tendency of water molecules.[28] It is thought that the water molecules form ordered structures around the side chains. As the temperature is increased the hydrogen bonding interactions grow weaker and the hydrophobic interactions of the isopropyl groups dominate and collapse the polymer structure.[29]

A cross-linked network the PNIPAm network will swell in the presence of water below the LCST. The swelling ratio is determined by the cross-link density of the PNIPAm network. Above the LCST, water is expelled from the hydrogel and the hydrogel collapses.[30]

Free-standing cross-linked PNIPAm hydrogels have been extensively investigated and a wide variety of shapes have been shown in previous studies.[14,30–33] Studies have also been conducted into surface-attached PNIPAm hydrogels investigating constrained swelling of PNIPAm hydrogels.[8,10,29,34,35] Few studies created cross-link density differences in the surface-attached films getting a surface structured hydrogel that is temperature responsive. However these hydrogel films are synthesized by polymerizing and cross-linking monomers by radical polymerization, which is sensitive to oxygen inhibition and are fabricated using in glass cells.[7,9,11,12] This limits these methods for coating larger surfaces and more complex surfaces then a flat glass substrate.

In this study we show a new method to create switchable surface structured hydrogel coatings. The polymer coating is made from a terpolymer based on PNIPAm that contains a co-monomer that acts as a photo-cross-linker: benzophenone acryl amide (BPAm). The polymer coatings are coated on a single substrate *via* industrial coating techniques *i.e.* slit die coating. The polymer is cross-linked in air, eliminating the need for an inert atmosphere.[32] By using multiple UV illumination steps we show that the swelling ratio can be locally varied, resulting in surface structures on the hydrogel at temperatures below

[a] *Dept. of Chemical Engineering and Chemistry, Functional Organic Materials & Devices (SFD), Eindhoven University of Technology, Building 14 – HELIX STO 0.26, De Rondom 70 – 5612 AP, P.O. Box 513 – 5600 MB, Eindhoven, The Netherlands. E-mail: s.kommeren@tue.nl*
[b] *Institute for Organic Chemistry, Johannes Gutenberg-University Mainz, Duesbergweg 10-14, D-55099 Mainz, Germany*
[c] *School of Engineering and Materials Science, Queen Mary University of London, Mile End Road, London E1 4NS, UK*

the LCST. When the temperature of the water is increased above the LCST the hydrogel expels water and collapses to a flat state.

2. Materials and methods

Synthesis of benzophenone acrylamide

Benzophenone acryl amide (BPAm) was synthesized according to the method of Kim *et al.*[30] Briefly, 4-aminobenzophenone (Sigma-Aldrich) (1.0 g, 5.07 mmol), acryloyl chloride (Sigma Aldrich) (453 μL, 5.56 mmol) and triethylamine (Sigma-Aldrich) (777 μL, 5.57 mmol) were dissolved in 10 mL of anhydrous dichloromethane (DCM, Biosolve). The solution was stirred for three hours and subsequently extracted three times each with 1 M HCl, saturated $NaHCO_3$, and finally with demineralized water. The extracted solution was dried using Na_2SO_4 and the DCM was evaporated by rotary evaporation. The remaining solid was purified by column chromatography on silica gel using 70% *n*-hexane: 30% ethyl acetate mixture as eluent. BPAm was obtained as a white solid. The product was dried at 40 °C overnight (yield 72%). ^{1}H-NMR ($CDCL_3$, 600 MHz): δ = 7.89 (s, N–*H*), 7.83 (m, 6× C*H* arom.), 7.58 (tt, J = 3, 11 Hz, 1× C*H* arom.), 7.47 (t, 11 Hz, 2× C*H* arom.), 6.47 (dd, J = 2, 25 Hz, CH_2═CH), 6.33 (dd, J = 16, 26 Hz, CH_2═CH), 6.29 (dd, J = 2, 15 Hz, CH_2═CH).

Synthesis of terpolymer

For our experiments, three different monomers were used: NIPAm, BPAm and acrylic acid (AAc). Each monomer has a different function for the polymer: NIPAm is temperature responsive, BPAm is a photo-cross-linker and AAc increases the hydrophilicity of the polymer. The resulting terpolymer is poly(NIPAM-*co*-BPAm-*co*-AAc) (PNBA).

The synthesis is done for the following mol ratios of the monomers: 92.3 mol% NIPAm, 1.9 mol% BPAm and 5.8 mol% AAc. In a round bottom flask 4.0 g NIPAm, 161 mg AAc, 183 mg BPAm and 11.8 mg of azobisisobutyronitrile (AIBN) initiator were dissolved in 40 mL 1,4-dioxane. After three cycles of freeze–pump–thaw and nitrogen purge the solution was heated to 80 °C in an oil bath overnight. The 1,4-dioxane solution was precipitated in cold diethyl ether and filtered with a büchner funnel. The remaining solvent was evaporated under reduced pressure to give a white solid. The terpolymer was subsequently dried in a vacuum oven overnight at 65 °C. ^{1}H-NMR (THF d8, 400 MHz): δ = 10.02 (s, OH), 7.78 (m, 6× C*H* arom.), 7.51 (m, 3× C*H* arom.), 7.18 (s, N*H*), 4.86 (s, N*H*), 4.02 (m, NH–C*H*–C_2H_6), 2.82–1.67 (3× m, polymer backbone), 1.16 (m, 2× CH–CH_3)(Fig. 1).

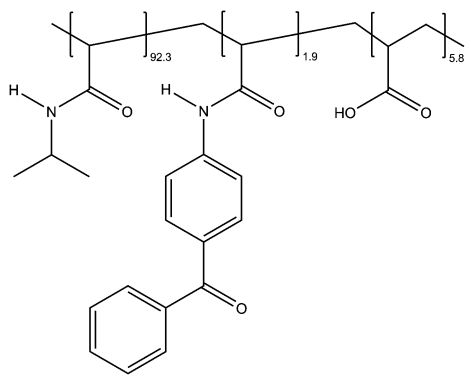

Fig. 1 The chemical structure of the photo-cross-linkable and temperature responsive terpolymer.

Substrate preparation

Glass substrates were cleaned by sonication (acetone, 15 min), and subsequently treated in an UV-ozone oven (Ultra Violet Products, PR-100, 20 min). The surface of the glass substrates were modified by spin coating a solution of 3-(trimethoxysilyl)-propyl acrylate (1% v/v in a water/isopropanol mixture, 1 : 1) onto the activated glass substrate for 30 sec at 3000 rpm. After curing for 10 min at 110 °C, the substrates were ready for use.

Sample preparation

The terpolymer was dissolved in a 1 : 2 ratio in ethanol and coated onto the prepared glass substrates with a RK K control coater (slit size: 200 μm). The PNBA film was then dried for 10 min at 100 °C. The terpolymer film was subsequently photo-cross-linked using UV light (Omnicure S2000, UVA range: 320–390 nm) at an intensity of 25 mW cm^{-2} until a total energy dose of 1, 2.5, 5, 10, 25, 50 or 100 J cm^{-2} was achieved. For the line patterns two subsequent illumination steps were used. First the film was illuminated with a mask until the desired cross-link density difference between the areas was achieved. Then the mask was removed and the entire PNBA film is illuminated to cross-link the whole film to the desired cross-link densities.

For the ratchet-like surface structures PNBA film was mask illuminated with an energy dose of 25 J cm^{-2} and subsequently the entire film was illuminated with a small energy dose of 2.5 J cm^{-2} to cross-link non-illuminated areas. Subsequent to the illumination procedure the PNBA films are swollen in demineralized water at room temperature (23 °C). For a more complex surface topography a three step illumination procedure was done. A line mask with a pitch of 150 μm is used in both of the mask illumination steps. In the first step the PNBA film is illuminated with an energy dose of 2.5 J cm^{-2}, then the mask is turned 90 degrees and in the second step the PNBA film is illuminated with an energy dose of 5 J cm^{-2}. For the last step the mask is removed and the whole PNBA film is illuminated with a final energy dose of 2.5 J cm^{-2}. This will results in four different areas with 2.5, 5, 7.5 and 10 J cm^{-2}.

Sample characterization

The absorption spectra were measured with UV spectrophotometer (Shimadzu, UV-3102 PC). The thickness of surface-attached PNBA films were measured with a confocal microscope Sensofar Plμ 2300 in combination with an 20× immersion objective (Nikon, CFI Fluor 20XW). The immersion objective allows for measurements in an aqueous environment. To increase the reflectance of the hydrogel surface a very thin gold layer (15 nm) is sputter coated (Emitech K550, 25 mA, 2 minutes) on the PNBA film. The PNBA films were first measured in the dry state and subsequently a water droplet is put on the entire PNBA film

and the objective is immersed in the water droplet. The PNBA film is left to equilibrate for 15 minutes, before each measurement. A hot stage (Linkam, THMS600) is placed underneath the sample to control the temperature. To determine the swelling ratio as a function of temperature the hot stage was gradually heated with steps of 0.5 °C from 23 °C (room temperature) to 50 °C. The hot stage is used to switch between 23 °C and 50 °C. The temperature cycles were repeated for several cycles, with a minimum of three cycles. Because the total amount of swelling is dependent on the thickness of the PNBA film the thickness measurements of the wet films are normalized to a swelling ratio, defined thickness of hydrogel film in water (swollen thickness) to that in air (dry thickness).

3. Results and discussion

In this study hydrogel coatings were created based on a PNIPAm terpolymer. The advantage of using a polymer is that the application of the coating can be done at ambient conditions by a variety of techniques *e.g.*; slit die coating or spray coating. This would not be possible when hydrogels are made from monomers. The combination of the volatility of the monomers and the need for an inert atmosphere due to the radical polymerization, makes this not suitable for single substrate fabrication.[7,9–12] The terpolymer is poly(NIPAM-*co*-BPAm-*co*-AAc) (PNBA) and consists of NIPAm, BPAm and acrylic acid (AAc). NIPAm gives the terpolymer its temperature responsive properties, BPAm is a photo-cross-linker and AAc increases the hydrophilicity of the terpolymer.[30,33]

The BPAm is a photo-cross-linker that cross-links polymer chains upon UV illumination. UV light (~250–365 nm) triggers an n–π* transition in BPAm that results in a diradical species. The diradical species abstracts a hydrogen from a neighbouring aliphatic group creating a stable C–C bond.[29,34–36] The absorption spectra of homogeneously illuminated PNBA films with different energy doses of UV light are shown in Fig. 2A. In the absorption spectra, it can be seen that the BPAm peak at 300 nm decreases with increasing energy dose, indicating that BPAm is being converted and that the PNBA is cross-linked. The arising peak at 250 nm is contributed to the less conjugated reaction product of BPAm after recombination.[32]

The temperature-induced phase transition of a swollen to a non-swollen state of the surface-attached PNBA hydrogels was investigated by measuring the thickness of the hydrogel films at various temperatures between room temperature (23 °C) and 50 °C. The thickness of the hydrogel coating is measured using *in situ* confocal microscopy in conjunction with an immersion objective. This enables one to characterize the thickness of the hydrogel films locally on a micrometre scale, which is not possible with other techniques like *e.g.* ellipsometry or neutron reflectometry.[8,10]

The swelling ratio is defined as the thickness of the hydrogel film in water (swollen thickness) to that in air (dry thickness). The swelling of the hydrogels was determined by measuring the thickness of the hydrogel film with confocal microscopy for different energy doses and/or temperatures.

In Fig. 3A, the swelling ratio of a hydrogel film that was homogenously cross-linked, with an energy dose of 2.5 J cm^{-2}, is plotted as a function of temperature. It can be seen that the swelling ratio is dependent on the temperature. Upon increasing the temperature, the hydrogen bonding interactions become weaker and the hydrophobic interactions of the isopropyl groups dominate and collapse the polymer structure decreasing the swelling ratio.[29] At high temperatures far above the LCST, a swelling ratio of 1.1 is found. It appears that the water is not entirely excluded from the collapsed PNBA hydrogel, which is in agreement with previous studies.[8,10,37] For further experiments we continue with 23 °C and 50 °C only, since this results in the biggest difference in swelling ratio.

Previously, studies have shown that there a direct relationship exists between the cross-link density and the swelling ratio of a hydrogel.[29,30,35] In Fig. 3B the swelling ratios of different homogenously cross-linked PNBA hydrogels are plotted against the energy dose. It is shown that the swelling ratio is dependent

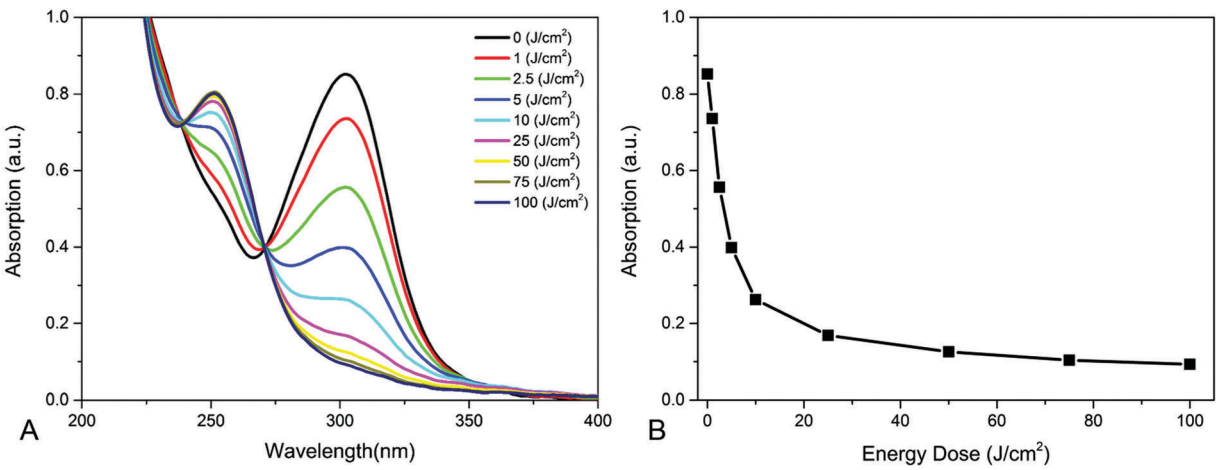

Fig. 2 (A) UV absorption spectra of a 2 μm thick PNBA film. The absorption peak of BPAm at 300 nm decreases with increasing energy dose. (B) The intensity of the absorption peak at 300 nm as a function of the energy dose.

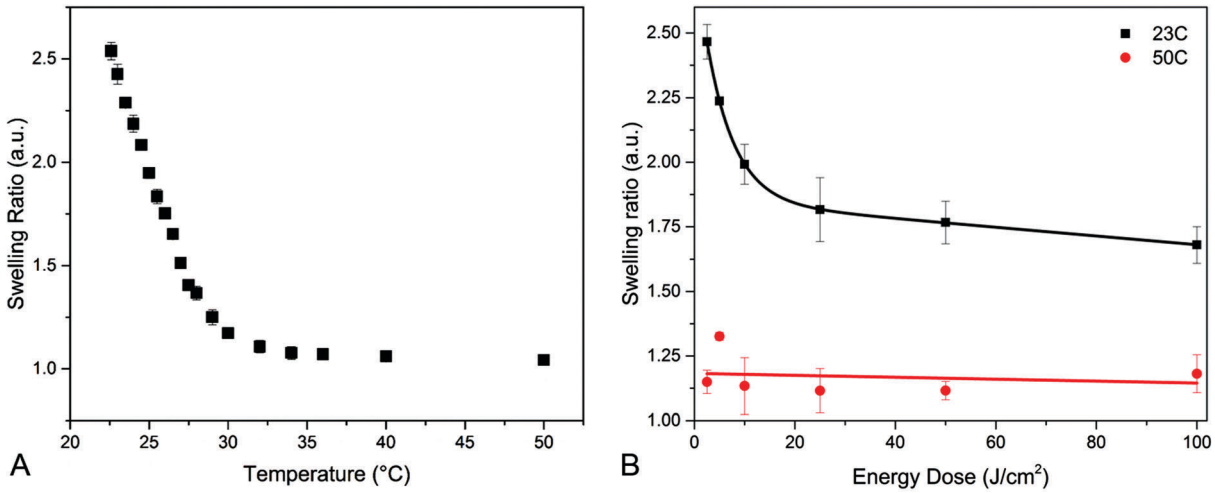

Fig. 3 (A) The swelling ratio of a homogenously cross-linked PNBA film is shown as a function of the temperature. (B) It is shown that the swelling ratio at 23 °C is dependent on the energy dose. Note that swelling ratio of the hydrogels at 50 °C is independent on the energy dose.

on the energy dose. In fact, a direct relationship is observed with the UV absorption of PNBA films. Which confirms that an increase in conversion of BPAm results in a higher cross-link density, which in turn results in a lower swelling ratio for the PNBA network.

In Fig. 3B the swelling ratio is also shown above the LCST (50 °C). It can be seen that the swelling ratio above the LCST is not dependent on the energy dose. This indicates that the collapse of the PNBA hydrogel network is not affected by the cross-link density.[29,34,37] An example of the swelling and collapse of a hydrogel film cross-linked with 2.5 J cm^{-2} is shown in Fig. 4A. In Fig. 4B, it is shown that the swelling and collapse of the hydrogel coating is reversible over several temperature cycles.

From the homogenously cross-linked hydrogels it can be concluded that the swelling ratio is dependent on energy dose at 23 °C. However the swelling ratio is independent of the energy dose at 50 °C. The combination of these properties is used to create a switchable surface structure. For example two adjacent areas could be illuminated with 2.5 J cm^{-2} and 50 J cm^{-2}, respectively. When swollen in water at 23 °C the area with low cross-link density swells to a swelling ratio of 2.5, while the area with high cross-link density swells to a swelling ratio of 1.8. This will result in a height difference between two areas. According to the swelling ratios found for homogenously cross-linked films (Fig. 3B), both areas will collapse upon heating to a swelling ratio of 1.1, resulting in a flat surface. This shows it is possible to create a hydrogel surface that is switchable between a flat and a structured state. To create such a switchable surface structure a two-step illumination is used to locally create different swelling ratios.

In the first step the PNBA film is illuminated through a mask until the desired cross-link density difference is achieved.

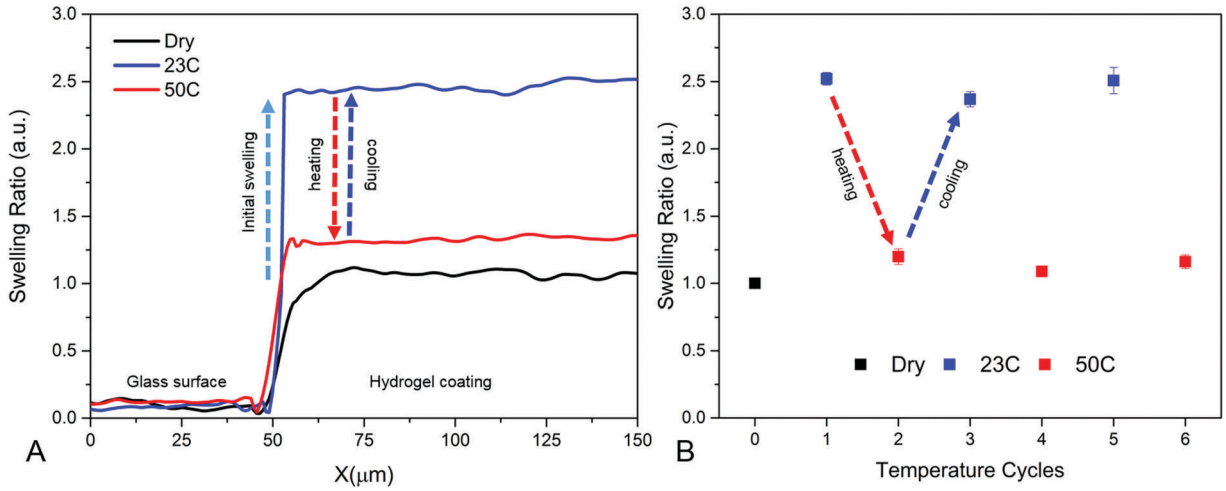

Fig. 4 The swelling ratios are measured *in situ* with a confocal microscope for a homogenously cross-linked (2.5 J cm^{-2}) PNBA film, with an initial thickness of 8 μm, at different temperatures. In (A) the PNBA film is shown prior to swelling (black), after swelling in 23 °C water (blue) and in 50 °C water (red). (B) The hydrogel can be switched between the two different swelling ratios over several temperature cycles.

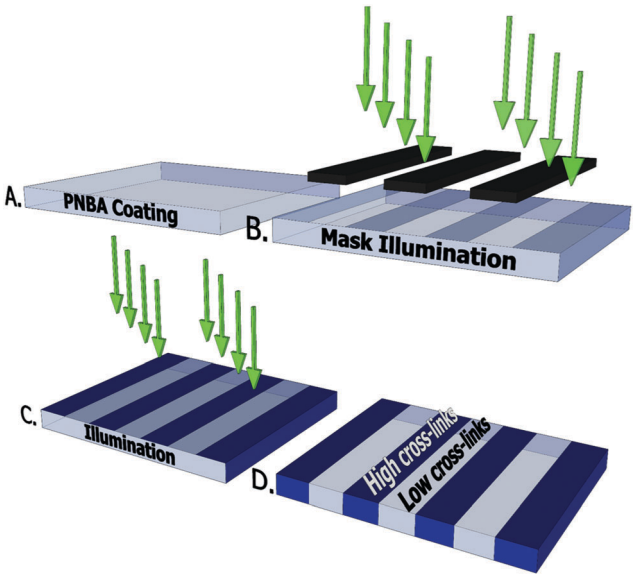

Fig. 5 Schematic representation of the UV illumination procedure. The PNBA film is first illuminated through a mask and subsequently the entire PNBA film illumination to create different cross-link densities throughout the film.

Subsequently the entire PNBA film is illuminated until the overall cross-link densities are obtained. The illumination procedure is schematically shown in Fig. 5.

Two areas are illuminated with a high energy dose (low swelling ratio) of 50 J cm^{-2} and to a low energy dose (high swelling ratio) of 2.5 J cm^{-2}. In the two-step illumination procedure a line mask with a pitch of 150 μm was used.

In Fig. 6A there are two areas with different swelling ratios upon swelling in water at 23 °C. And, as with homogenously cross-linked hydrogels, both areas collapse to a swelling ratio of 1.1 when heated to 50 °C resulting in a flat film. It has to be noted that in Fig. 6A the axis are not proportional therefore the surface structures may appear higher than in reality. In Fig. 6B, it is shown that this process is reversible over several temperature cycles. This shows it is possible to create a switchable surface structured hydrogel coating.

In the example in Fig. 6 the lowest energy dose (2.5 J cm^{-2}) was used to create surface structures as high as possible. It was shown in Fig. 3B the swelling ratio is dependent on the energy dose. By controlling the energy dose difference between areas the height of the surface structures can be varied. In Fig. 7 the swelling ratio difference between the two areas is shown as a function of the energy dose difference. As expected the height of the surface structure decreases when the difference in energy dose decreases.

With this tunable property in mind, one can imagine that more complex patterns are possible then a simple line pattern

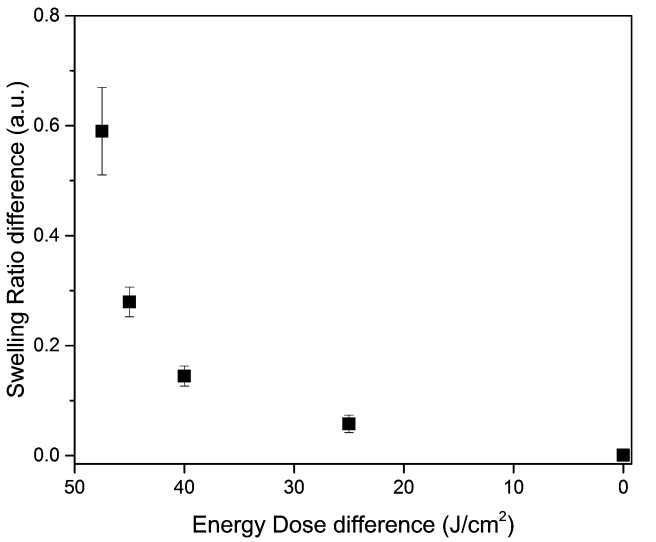

Fig. 7 The swelling ratio difference is shown as a function of the energy dose difference of the separate areas.

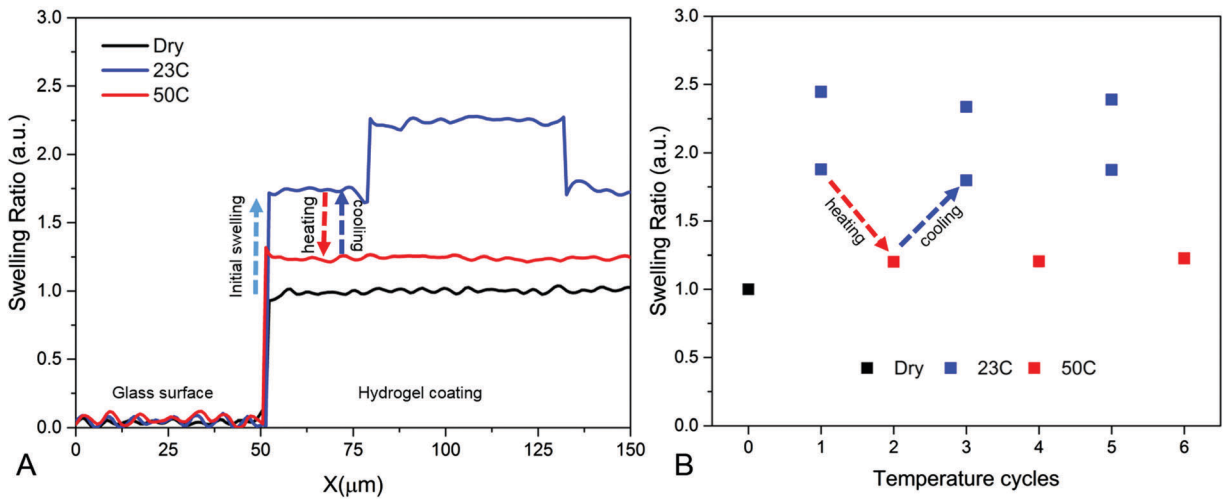

Fig. 6 The swelling ratios are measured *in situ* with a confocal microscope for a patterned photo-cross-linked (2.5 and 50 J cm^{-2}) PNBA film, with an initial thickness of 10 μm, at different temperatures. In (A) the PNBA film is shown prior to swelling (black), after swelling in 23 °C water (blue) and in 50 °C water (red). The PNBA hydrogel can be switched between a structured state with two distinct swelling ratio areas at 23 °C and a flat state were the whole PNBA film collapses to one swelling ratio at 50 °C. In (B) it is shown that this switching behaviour is stable over several temperature cycles.

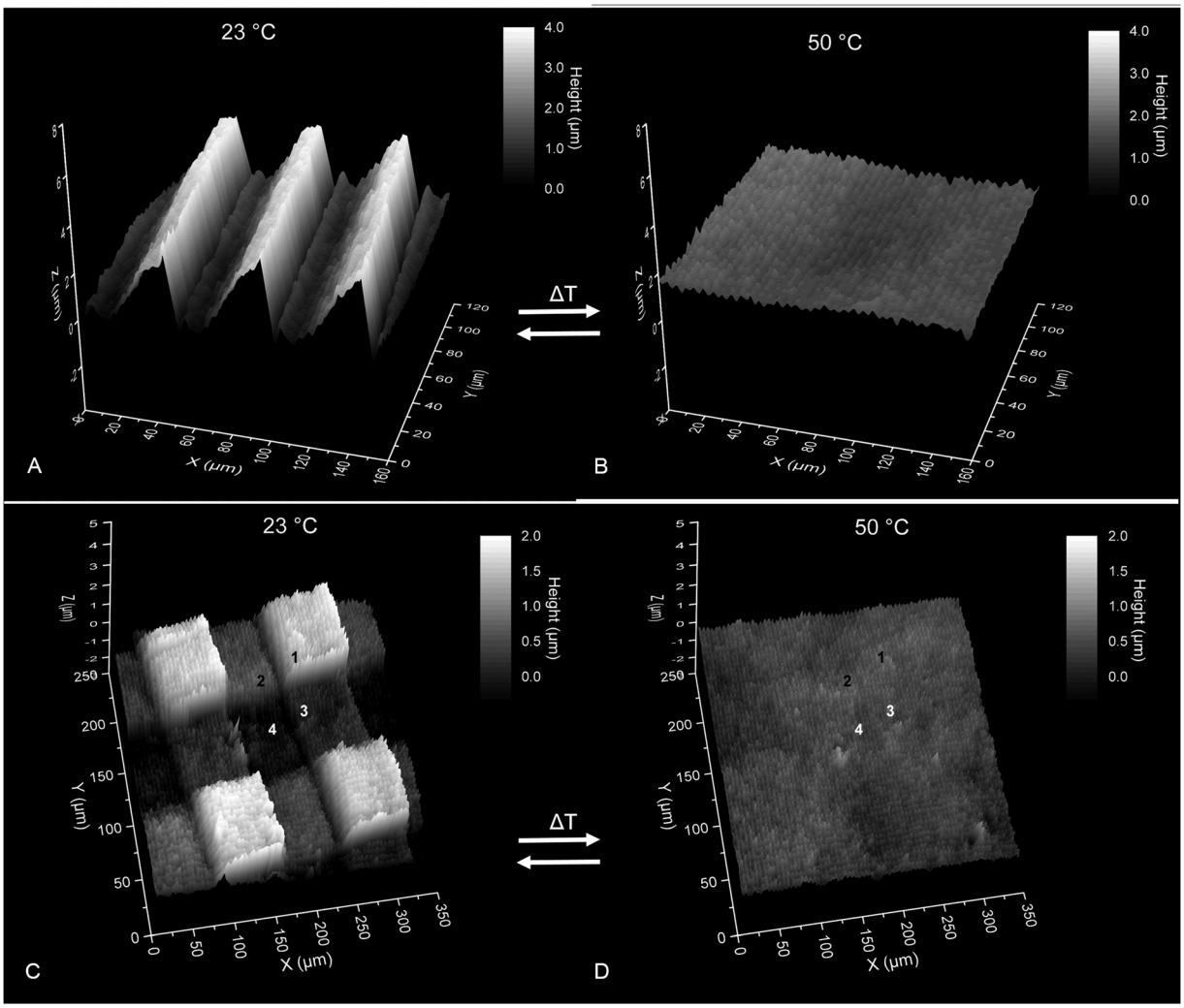

Fig. 8 (A) A ratchet-like surface structure is obtained through illumination with a grayscale mask. (B) The ratchet-like surface structure disappears completely when the temperature is increased above the LCST. (C) A square pattern is observed with four different heights, due to a three step illumination procedure. (D) Again the pattern disappears completely upon increasing the temperature above the LCST.

as shown in Fig. 6. To show this illumination process is not limited to a simple line pattern two examples of more complex surface structures are shown in Fig. 8. The first example uses a grayscale mask with a pitch of 50 μm and linearly varies over the length of the pitch from 100% transmission to 0% transmission. Due to the variation in transparency the energy dose will vary over the length of the mask pitch and in turn the swelling ratio will vary over the length of the mask pitch. Therefore a ratchet-like structure is expected upon swelling of the PNBA film in water. In Fig. 8A, it can be seen that a ratchet-like surface structure was indeed obtained and this surface structure can even be switched back to a flat surface by increasing the temperature above the LCST, see Fig. 8B.

The second example of a more complex surface structure is made by multiple subsequent UV mask illuminations steps. This results in four areas that have a different energy dose namely: 2.5, 5, 7.5 and 10 J cm^{-2} the areas are noted as 1, 2, 3 and 4, respectively. Note that the energy dose of each UV illumination step can be added together to get the final energy dose of a particular area. This would not be possible when using polymerization induced diffusion where polymerization is initiated immediately upon UV illumination.

In Fig. 8C, it is shown that a square pattern in obtained when the film is submerged in water and four different heights are observed (annotated with the numbers 1 to 4). In Fig. 8D the sample is heated above the LCST and it shows that the height difference between the four areas disappears. Note that in both examples that the axis are not proportional *i.e.* aspect ratios of the features appear higher than in reality. This again confirms the results from the homogenously cross-linked hydrogel coatings: the swelling ratio above the LCST is independent of the energy dose. In both of the examples the surface structures could be switched 'on' and 'off' multiple times.

The complex surface structures in hydrogel coatings shows the versatility of the photo-cross-linking method described here. More common techniques, like polymerization induced diffusion, are limited to one mask UV illumination step limiting the complexity of the surface structures in the hydrogel coating.[7,9,11]

This tunability combined with the ease of application of the photo-cross-linkable polymer makes it a very versatile method for making surface structures in hydrogel coatings.

4. Conclusions

We have described a novel method for preparation of switchable surface structures in hydrogel coatings. The creation of the surface structures relies on the non-uniform swelling in temperature responsive PNIPAm hydrogel coatings. The system is based on selective photo-cross-linking between polymer chains. The advantage of using a polymer is that the application of the coating can be done at ambient conditions by an industrial coating techniques like: slit die coating. This gives the freedom of coating on a single substrate without the need for glass moulds or other methods to contain monomers. The polymer is made from NIPAm, a photo-cross-linker: benzophenone acrylamide (BPAm) and acrylic acid (AAc).

It is shown that the PNBA terpolymer can create a cross-links by UV illumination. The amount of cross-links can be controlled with the energy dose of the UV illumination. This in turn results in a control over the swelling ratio as the conversion of BPAm is directly related to the amount of cross-linking in the polymer network. Simple and complex surface structures were created using, respectively, single or multiple UV illumination steps through masks resulting in surface structures on the hydrogel coatings and it was shown that the hydrogel coatings can be reversibly switched from a structured state to a flat state with temperature.

Acknowledgements

The Authors would like to gratefully acknowledge the financial support of the EU-FP7-SEAFRONT project (614034). The Authors would particularly like to acknowledge M. P. F. H. L. van Maris for his help with the experimental setup for the *in situ* confocal microscope setup and discussion thereof.

References

1 L. Dong, A. K. Agarwal, D. J. Beebe and H. Jiang, *Nature*, 2006, **442**, 551–554.
2 L. T. de Haan, J. M. N. Verjans, D. J. Broer, C. W. M. Bastiaansen and A. P. H. J. Schenning, *J. Am. Chem. Soc.*, 2014, **136**, 10585–10588.
3 G. N. Mol, K. D. Harris, C. W. M. Bastiaansen and D. J. Broer, *Adv. Funct. Mater.*, 2005, **15**, 1155–1159.
4 D. Liu and D. J. Broer, *Soft Matter*, 2014, **10**, 7952–7958.
5 R. A. Barry and P. Wiltzius, *Langmuir*, 2005, **22**, 1369–1374.
6 M. R. Islam and M. J. Serpe, *RSC Adv.*, 2014, **4**, 31937–31940.
7 D. Liu, C. W. M. Bastiaansen, J. M. J. den Toonder and D. J. Broer, *Soft Matter*, 2013, **9**, 588–596.
8 B. Chollet, L. D'Eramo, E. Martwong, M. Li, J. Macron, T. Q. Mai, P. Tabeling and Y. Tran, *ACS Appl. Mater. Interfaces*, 2016, **8**, 24870–24879.
9 D. Liu, C. W. Bastiaansen, J. M. den Toonder and D. J. Broer, *Langmuir*, 2013, **29**, 5622–5629.
10 M. Li, B. Bresson, F. Cousin, C. Fretigny and Y. Tran, *Langmuir*, 2015, **31**, 11516–11524.
11 J. E. Stumpel, D. Liu, D. J. Broer and A. P. Schenning, *Chemistry*, 2013, **19**, 10922–10927.
12 J. E. Stumpel, B. Ziółkowski, L. Florea, D. Diamond, D. J. Broer and A. P. H. J. Schenning, *ACS Appl. Mater. Interfaces*, 2014, **6**, 7268–7274.
13 T. Satoh, K. Sumaru, T. Takagi and T. Kanamori, *Soft Matter*, 2011, **7**, 8030–8034.
14 A. W. Hauser, A. A. Evans, J. H. Na and R. C. Hayward, *Angew. Chem.*, 2015, **54**, 5434–5437.
15 D. J. Beebe, J. S. Moore, J. M. Bauer, Q. Yu, R. H. Liu, C. Devadoss and B.-H. Jo, *Nature*, 2000, **404**, 588–590.
16 S. Sugiura, K. Sumaru, K. Ohi, K. Hiroki, T. Takagi and T. Kanamori, *Sens. Actuators, A*, 2007, **140**, 176–184.
17 M. Nakayama, N. Yamada, Y. Kumashiro, H. Kanazawa, M. Yamato and T. Okano, *Macromol. Biosci.*, 2012, **12**, 751–760.
18 L. K. Ista, *J. Ind. Microbiol. Biotechnol.*, 1998, **20**, 121–125.
19 M. E. Nash, W. M. Carroll, P. J. Foley, G. Maguire, C. O. Connell, A. V. Gorelov, S. Beloshapkin and Y. A. Rochev, *Soft Matter*, 2012, **8**, 3889–3899.
20 G. de Vicente and M. C. Lensen, *Eur. Polym. J.*, 2016, **78**, 290–301.
21 J. D. Kiang, J. H. Wen, J. C. del Álamo and A. J. Engler, *J. Biomed. Mater. Res., Part A*, 2013, **101**, 2313–2321.
22 M. Nikkhah, F. Edalat, S. Manoucheri and A. Khademhosseini, *Biomaterials*, 2012, **33**, 5230–5246.
23 W.-K. Lee, L. J. Whitman, J. Lee, W. P. King and P. E. Sheehan, *Soft Matter*, 2008, **4**, 1844–1847.
24 G. Joseph, J. Pichardo and G. Chen, *Analyst*, 2010, **135**, 2303–2308.
25 H. E. H. Meijer, M. K. Singh, T. G. Kang, J. M. J. den Toonder and P. D. Anderson, *Macromol. Symp.*, 2009, **279**, 201–209.
26 M. Lei, Y. Gu, A. Baldi, R. A. Siegel and B. Ziaie, *Langmuir*, 2004, **20**, 8947–8951.
27 H. G. Schild, *Prog. Polym. Sci.*, 1992, **17**, 163–249.
28 Y. Maeda, T. Nakamura and I. Ikeda, *Macromolecules*, 2001, **34**, 1391–1399.
29 A. Vidyasagar, J. Majewski and R. Toomey, *Macromolecules*, 2008, **41**, 919–924.
30 J. Kim, J. A. Hanna, M. Byun, C. D. Santangelo and R. C. Hayward, *Science*, 2012, **335**, 1201–1205.
31 M. Byun, C. D. Santangelo and R. C. Hayward, *Soft Matter*, 2013, **9**, 8264–8273.
32 S. K. Christensen, M. C. Chiappelli and R. C. Hayward, *Macromolecules*, 2012, **45**, 5237–5246.
33 J. Kim, J. A. Hanna, R. C. Hayward and C. D. Santangelo, *Soft Matter*, 2012, **8**, 2375–2381.
34 R. Toomey, D. Freidank and J. Rühe, *Macromolecules*, 2004, **37**, 882–887.
35 A. Vidyasagar, H. L. Smith, J. Majewski and R. G. Toomey, *Soft Matter*, 2009, **5**, 4733–4738.
36 V. Carias, J. Wang and R. Toomey, *Langmuir*, 2014, **30**, 4105–4110.
37 D. Kuckling, M. E. Harmon and C. W. Frank, *Macromolecules*, 2002, **35**, 6377–6383.